THE ONSET OF CONVECTIVE INSTABILITY IN AN ANISOTROPIC POROUS MEDIUM LAYER WITH INTERNAL HEATING AND VARYING GRAVITY

LLEGADA DE LA ACTIVIDAD DE CONVECCIÓN EN UNA CAPA POROSA ANISOTRÓPICA CON CALENTAMIENTO INTERNO Y EFECTOS GRAVITATORIOS INCONSISTENTES

D. Yadav[a†]

Department of Mathematical & Physical Sciences, University of Nizwa, P.O.B.-616, Oman; dhananjayadav@gmail.com
† corresponding author

Recibido 25/1/2020; Aceptado 17/6/2018

In this article, the impact of consistent internal heat source and varying downward gravity force on the onset of convective movement in an anisotropic porous matrix is studied numerically applying the high-term Galerkin technique. The gravity field variations with depth z are considered to be of four types: (a) $G(z) = -z$, (b) $G(z) = -z^2$, (c) $G(z) = -z^3$, and (d) $G(z) = -(e^z - 1)$. Outcomes show that both the thermal anisotropy parameter η and gravity variation parameter λ delay the onset of convection, while the internal heating parameter Hs and the mechanical anisotropy parameter ξ speed up the arrival of convective activity. The dimension of the convection cells boosts with η, ξ and λ, while it diminishes with Hs. It is also identified that the system shows maximum stability for case (d), while it is minimum for case (c).

En este artículo se estudia numéricamente el impacto de una fuente de calor interna y una fuerza de gravedad variable que apunta hacia abajo, sobre el comienzo de la convección en una matriz porosa anisotrópica, aplicando la técnica de términos alto de Galerkin. La variación del campo gravitatorio con la profundidad z se considera de cuatro tipos: (a) $G(z) = -z$, (b) $G(z) = -z^2$, (c) $G(z) = -z^3$, y (d) $G(z) = -(e^z - 1)$. Los resultados muestran que tanto el parámetro de anisotropía térmica η como el de variación de la gravedad λ retrasan el comienzo de la convección, mientras que el parámetro de calentamiento interno Hs y el de anisotropía mecánica ξ aceleran el comienzo de la actividad convectiva. La dimensión de las celdas de convección aumenta η, ξ y λ, mientras que decrece Hs. También se observa que el sistema muestra máxima estabilidad para el caso (d), y mínima para (c).

PACS: Convection (convección), 44.25.+f; Thermal convection (fluid dynamics) (convección térmica (dinámica de fluidos)), 47.55.pb; Porous materials, flow thorugh (materiales porosos, flujo a través), 47.56.+r

I. INTRODUCTION

Convective instability in a porous medium, associated to buoyancy due to temperature gradients, has attracted strong interest in the past as well as nowadays because of its many applications. They include underground transport of impurities, chilling of electronic components, the underground exclusion of nuclear waste, petroleum drilling, chemical and food practicing [1–6]. The study of the onset of convective flow in a porous layer starts with the Horton-Rogers-Lapwood (HRL) instability problem [7]. There, the authors studied heat driven convection and obtained that the critical Darcy-Rayleigh number is $4\pi^2$. The extension of the classical HRL convection problem was well reviewed by Nield and Bejan [8].

Anisotropy in porous media, which arises from non-symmetrical pattern of porous matrix or fibres, is commonly found in nature and in many engineering applications. Rock, soils and fibrous insulating materials are excellent instances of anisotropic porous media. The thermal instability in a layer of porous matrix with anisotropic permeability was originally studied by Castinel and Combarnous [9]. They obtained the conditions on the start of convection experimentally as well as theoretically. Epherre [10] extended the instability examination to a porous medium layer with anisotropic thermal diffusivity. Nonlinear instability due to a heat gradient in an anisotropic porous matrix was studied by Kvernvold and Tyvand [11]. They derived the criterion for the start of convection theoretically. Later, Degan *et al.* [12], Payne *et al.* [13], Rees and Postelnicu [14], Govinder [15], Malashetty and Swamy [16], Yadav and Kim [17], Shivakumara et al. [18] and Mahajan and Nandal [19] extended this problem to the cases of vertical anisotropic porous layer, anisotropic permeability on Darcy's law, inclined anisotropic porous layer, Coriolise effect, duble diffusive convection, transient convective activities, local thermal non-equilibrium and Brinkman effects, respectively.

The impact of internal heating plays a very important character on the thermal convection in porous media due to its natural occurrence as well as its importance to control the convective motion in many engineering applications. A practical situation, in which a porous medium can have internal heat source, occurs in the underground removal of radioactive dissipate materials, geophysics, crystal growth, miniaturization of electronic components and exothermic chemical processes in packed-bed reactors. The power of internal warming on the onset of convection in a porous matrix was explored by Gasser and Kazimi [20]. They obtained the critical interior and outer Rayleigh numbers for the start of convective motion. Parthiban and Patil [21] investigated the convective activity in an asymmetric porous

layer with internal heating and inclined heat gradient. The effects of Darcy number and uniform heat supply on the onset of convection in a porous medium layer was studied by Nouri-Borujerdi *et al.* [22]. Bhadauria et al. [23] examined the significance of rotation on the start of convection in an anisotropic porous layer with internal heat generation by a weak nonlinear analysis. Very recently, Storesletten and Rees [24] researched the onset of convection in an inclined anisotropic porous layer persuaded by a constant distribution of internally heat sources. For more details on the onset of convection with internal warm source, we refer the reader to references [25–35].

Although most studies related to convective instability are concerned with constant gravity field, convection due to a varying gravity field has received small attention. However, there are many convective conditions that exist in science and engineering such as large scale flows in the Earth's crust and in crystals growth where the variation of gravity with depth in the apparatus is important [36–39]. Therefore, the analysis of fluid convection with changeable gravity appears essential. Kaloni and Qiao [40] examined the arrival of heat convection in a porous matrix with inclined thermal gradient and gravitational field which was changing linearly with depth in the layer. Alex et al. [41–43] extended their stability examination with throughflow, internal heat source and anisotropic. They detected that gravity increasing upwards is a destabilizing influence. Rionero and Straughan [44] presented the convective instability in a porous matrix with a uneven gravity field and heat source using linear and non-linear investigations. They studied three different categories of changeable gravity fields on the initiation of convective activity. The influence of magnetic force and gravity difference on the launch of convective movement in porous matrix was examined by Harfash [45]. Afterward, Mahajan and Sharma [46], Chand et al. [47] and Yadav [48] examined the influence of uneven gravitational force on the nanofluid convective motion. Very recently, Yadav [49] examined the significance of uneven gravity force and even throughflow on the start of convection in a Darcian porous medium and found that these parameters are to suspend the start of convective activity. The extension with rotation was also made by Yadav [50].

Due to the important applications of the internal heat source and the deviation of gravitational force with depth (linear, parabolic, binomial and exponential) in sedimentary basins, epeirogenic and orogenic activities of the Earth's crust, and crustal structures [51–53], in this article we examine the internal heat source effect on the onset of convection in a fluid saturated anisotropic porous medium layer with four types of gravitational force variation: (a) $G(z) = -z$, (b) $G(z) = -z^2$, (c) $G(z) = -z^3$, and (d) $G(z) = -(e^z - 1)$ numerically. The simulations are performed and explored for the internal heat source and the gravity deviation parameters on the arrival of convection via figures and tables.

II. MODELLING OF THE PROBLEM

An infinite parallel layer of fluid saturated anisotropic porous layer bounded among the limits $z = 0$ and $z = h$, and heated from below is considered. The layer is acted upon by a regular heat supply Q_0 and uneven gravitational field $g(z)$ which depends on the vertical aspect z and acts in the reverse z-way. The temperatures at the lower and upper boundaries are presumed to be θ_1 and θ_2 ($\theta_2 < \theta_1$), respectively. Under the assumptions of Darcy's law, the relevant governing equations are [25, 54, 55]:

$$\nabla \cdot \mathbf{u} = 0, \tag{1}$$

$$0 = -\nabla P - \mu \tilde{\mathbf{K}}^{-1}\mathbf{u} - \rho_0[1 - \beta(\theta - \theta_0)]g(z)\hat{\mathbf{e}}_z, \tag{2}$$

$$\left[(\rho c)_m \frac{\partial}{\partial \tau} + (\rho c)_f(\mathbf{u} \cdot \nabla)\right]\theta = \nabla \cdot (\tilde{\mathbf{k}}_m \cdot \nabla\theta) + Q_0. \tag{3}$$

Here, $g(z) = g_0[1 + \lambda G(z)]$ is the changeable gravity, $G(z)$ is the functional value for the uneven gravity field, θ is the temperature, g_0 is the reference density, λ is the gravity variation parameter, τ indicates the time, $\mathbf{u}$ indicates the velocity, ρ_0 indicates the density of fluid at reference temperature $\theta_2 = \theta_0$, μ indicates the viscosity, β indicates the thermal growth coefficient, $(\rho c)_f$ and $(\rho c)_m$ denote heat capacities of the fluid and effective porous matrix, $\tilde{\mathbf{K}}^{-1}$ and $\tilde{\mathbf{k}}_m$ are the converse of the permeability and the thermal conductivity tensors of the porous medium, respectively and defined as:

$$\tilde{\mathbf{K}}^{-1} = K_x^{-1}\hat{\mathbf{e}}_x\hat{\mathbf{e}}_x + K_y^{-1}\hat{\mathbf{e}}_y\hat{\mathbf{e}}_y + K_z^{-1}\hat{\mathbf{e}}_z\hat{\mathbf{e}}_z, \tag{4}$$

$$\tilde{\mathbf{k}}_m = k_{mx}\hat{\mathbf{e}}_x\hat{\mathbf{e}}_x + k_{my}\hat{\mathbf{e}}_y\hat{\mathbf{e}}_y + k_{mz}\hat{\mathbf{e}}_z\hat{\mathbf{e}}_z. \tag{5}$$

In this examination, we have taken the horizontal mechanical and thermal isotropy, i.e. $K_x^{-1} = K_y^{-1}$ and $k_{mx} = k_{my}$. The above governing Eqs. (1-3) are non-dimensionalized by taking the subsequent substitution:

$$\begin{cases} (x, y, z) = h(x, y, z), & \theta = \theta\Delta\theta + \theta_c, \qquad \mathbf{u} = k_\nu \mathbf{u}/h, \\ \tau = h^2\tau/k_\nu, & P = \mu_{nf}k_\nu P/K_z, \end{cases} \tag{6}$$

where $k_\nu = k_{mz}/(\rho c)$, $\Delta\theta = \theta_1 - \theta_2$. Then, non-dimensional form of Eqs. (1-3) after reduced the five unknowns u, v, w, P and θ to two (w and θ) by operating on Eq. (2) with $\hat{\mathbf{e}}_z \cdot \nabla \times \nabla \times$ are (after disregarding the tie superscripts for ease):

$$\nabla_H^2 w + \frac{1}{\xi}\frac{\partial^2 w}{\partial z^2} - R_D\nabla_H^2\theta[1 + \lambda G(z)] = 0, \tag{7}$$

$$\gamma\frac{\partial\theta}{\partial\tau} + (\mathbf{u} \cdot \nabla)\theta = \left(\eta\nabla_H^2 + \frac{\partial^2}{\partial z^2}\right)\theta + \mathrm{Hs}. \tag{8}$$

Here, $\nabla = \hat{\mathbf{e}}_x\partial/\partial x + \hat{\mathbf{e}}_y\partial/\partial y + \hat{\mathbf{e}}_z\partial/\partial z$, $\nabla_H^2 = \partial^2/\partial x^2 + \partial^2/\partial y^2$, $\xi = K_x/K_z$ represents the mechanical anisotropy parameter, $R_D = \rho_0\beta h K_z g_0\Delta\theta/(\mu k_{/nu})$ represents the thermal Rayleigh-Darcy number, $\mathrm{Hs} = h^2Q_0/(\Delta\theta(\rho c)_f k_\nu)$ represents the internal heating parameter, $\eta = k_{mx}/k_{mz}$ represents the thermal anisotropy parameter, and $\gamma = (\rho c)_m/(\rho c)_f$ represents the heat capacity ratio. The boundary conditions can be written as:

$$\begin{cases} w = 0, \quad \theta = 1, & \text{at } z = 0, \\ w = 0, \quad \theta = 0, & \text{at } z = 1. \end{cases} \tag{9}$$

The basic condition is assumed to be quiescent and of the form: $\mathbf{u}_b = (0,0,0)$, $\theta_b = \theta_b(z)$. Then the conduction status temperature is obtained as:

$$\theta_b = 1 - z - \frac{\mathrm{Hs}}{2} z(z-1). \tag{10}$$

III. STABILITY EQUATIONS

We assume the disturbance variables as $\mathbf{u} = \mathbf{u}_b + \mathbf{u}'$ and $\theta = \theta_b + \theta'$. Here $\mathbf{u}'$ and θ' indicate the perturbed measures from their basic situation and assumed to be very small. On inserting the above values of $\mathbf{u}$ and θ into Eqs. (7) and (8) and linearizing, we have the stability equations as:

$$\nabla_H^2 w' + \frac{1}{\xi}\frac{\partial^2 w'}{\partial z^2} = R_D \nabla_H^2 \theta' [1 + \lambda G(z)] = 0, \tag{11}$$

$$\gamma \frac{\partial \theta'}{\partial \tau} + (\mathbf{u}' \cdot \nabla)\theta_b + (\mathbf{u}_b \cdot \nabla)\theta' = \left(\eta \nabla_H^2 + \frac{\partial^2}{\partial z^2}\right)\theta'. \tag{12}$$

We assume the result of the perturbed quantities as [56–63]:

$$(w', \theta') = [\tilde{w}(z), \tilde{\theta}(z)] \exp i(\kappa x + \chi y) + \sigma\tau, \tag{13}$$

where κ and χ represent the horizontal wave numbers and σ represents the expansion rate of volatility. On application of Eq. (13) into Eqs. (11) and (12), we can write:

$$\left[\frac{1}{\xi} D^2 - a^2\right]\tilde{w} + a^2 R_D \tilde{\theta}[1 + \lambda G(z)] = 0, \tag{14}$$

$$-\frac{d\theta_b}{\theta z}\tilde{w} + [D^2 - \eta a^2 - \gamma\sigma]\tilde{\theta} = 0, \tag{15}$$

where $d/dz \equiv D$ and $a = \sqrt{\kappa^2 + \chi^2}$ represents the wave number. In the perturbation formation, the boundary states are:

$$\tilde{w} = \tilde{\theta} = 0, \qquad \text{at } z = 0, 1, \tag{16}$$

IV. SOLUTION TECHNIQUE

Galerkin procedure is employed to crack the arrangement of linear Eqs. (14) and (15). So the variables are assumed as:

$$\tilde{w} = \sum_{k=1}^{N} A_k \tilde{w}_k \qquad \text{and} \qquad \tilde{\theta} = \sum_{k=1}^{N} B_k \tilde{\theta}_k \tag{17}$$

Here A_k and B_k are constants and, $\tilde{w}_k$ and $\tilde{\theta}_k$ satisfy the boundary conditions (Eq. (16)) and assumed as $\tilde{w}_k = \tilde{\theta}_k = \sin k\pi z$. Using Eq. (17) into Eqs. (14) and (15) and applying the orthogonal characteristics, we have:

$$C_{jk} A_k + D_{jk} B_k = 0, \qquad E_{jk} A_k + F_{jk} B_k = \sigma G_{jk} B_k. \tag{18}$$

Here, $C_{jk} = \left\langle \frac{D\tilde{w}_j D\tilde{w}_k}{\xi} - a^2 \tilde{w}_j \tilde{w}_k \right\rangle$, $D_{jk} = \left\langle a^2 R_D \tilde{w}_j \tilde{\theta}_k [1 + \lambda G(z)] \right\rangle$, $E_{jk} = \left\langle -\tilde{\theta}_j \tilde{w}_k D\theta_b \right\rangle$, $F_{jk} = \left\langle D\tilde{\theta}_j D\tilde{\theta}_k - \eta a^2 \tilde{\theta}_j \tilde{\theta}_k \right\rangle$, $G_{jk} = \left\langle \gamma \tilde{\theta}_j \tilde{\theta}_k \right\rangle$, where $\langle YZ \rangle = \int_0^1 YZ\, dz$.

The collection of Eq. (18) forms a generalized eigenvalue position and resolved in Matlab using QZ process and EIG function. The critical thermal Rayleigh-Darcy number $R_{D,c}$, the critical wave number a_c and the critical value of the frequency of oscillations $\sigma_{i,c}$ are calculated using the golden search and Newton's methods. The nature of the convective motion is stationary for the taken problem.

V. RESULTS AND DISCUSSION

A numerical investigation has been made to inspect the influences of the uniform internal heat source and changeable gravity force on the arrival of instability in an anisotropic porous matrix. The problem is solved for four types of gravity field digression: (a) $G(z) = -z$, (b) $G(z) = -z^2$, (c) $G(z) = -z^3$, and (d) $G(z) = -(e^z - 1)$ using 6-terms Galerkin method [49]. The conditions for the start of instability is attained in forms of $R_{D,c}$ and a_c for a different variety of Hs, λ, ξ and η. According to Malashetty and Swamy [16], Shivakumara et al. [18], Mahajan and Nandal [19], Yadav [29] and Rionero and Straughan [44], we have considered the values of Hs in the order 10^2 and the value of λ in between 0 to 2. The values of ξ and η are not more than 1.

To prove the precision of the current outcomes, primary test imitations are made in the nonattendance of internal heat source and motion in isotropic porous matrix, i.e. Hs = 0, $\xi = \eta = 1$, and outcomes are good agreement with Rionero and Straughan [44] as shown in Table 1. This proves the accuracy of the method used.

Table 1. Contrast of the $R_{D,c}$ and the a_c with λ in the nonappearance of internal heat supply and flow in isotropic porous medium, i.e. Hs = 0, $\xi = \eta = 1$ for categories (a) $G(z) = -z$, (b) $G(z) = -z^2$, (c) $G(z) = -z^3$, and (d) $G(z) = -(e^z - 1)$.

		Current Study		Rionero and Straughan	
$G(z)$	λ	$R_{D,c}$	a_c^2	$R_{D,c}$	a_c^2
(a)	0.0	39.478	9.872	39.478	9.870
	1.0	77.080	10.208	77.020	10.209
	1.5	132.020	12.313	132.020	12.314
	1.8	189.908	17.198	189.908	17.198
	1.9	212.281	19.475	212.280	19.470
(b)	0.0	39.478	9.872	39.478	9.870
	0.2	41.832	9.872	41.832	9.874
	0.4	44.455	9.885	44.455	9.887
	0.6	47.389	9.916	47.389	9.915
	0.8	50.682	9.960	50.682	9.961
	1.0	54.390	10.036	54.390	10.034
(d)	0.0	39.478	9.872	39.478	9.870
	0.1	42.331	9.872	42.331	9.872
	0.2	45.607	9.885	45.607	9.883
	0.3	49.398	9.904	49.398	9.904
	0.4	53.828	9.941	53.828	9.942
	0.5	59.053	10.005	59.053	10.005

Fig. 1 exhibits the disparity of with for categories (a) $G(z) = -z$, (b) $G(z) = -z^2$, (c) $G(z) = -z^3$, and (d) $G(z) = -(e^z - 1)$ with diverse estimates of Hs. The corresponding a_c is shown in Fig. 2. The outcomes are also listed in Tables 2 and 3.

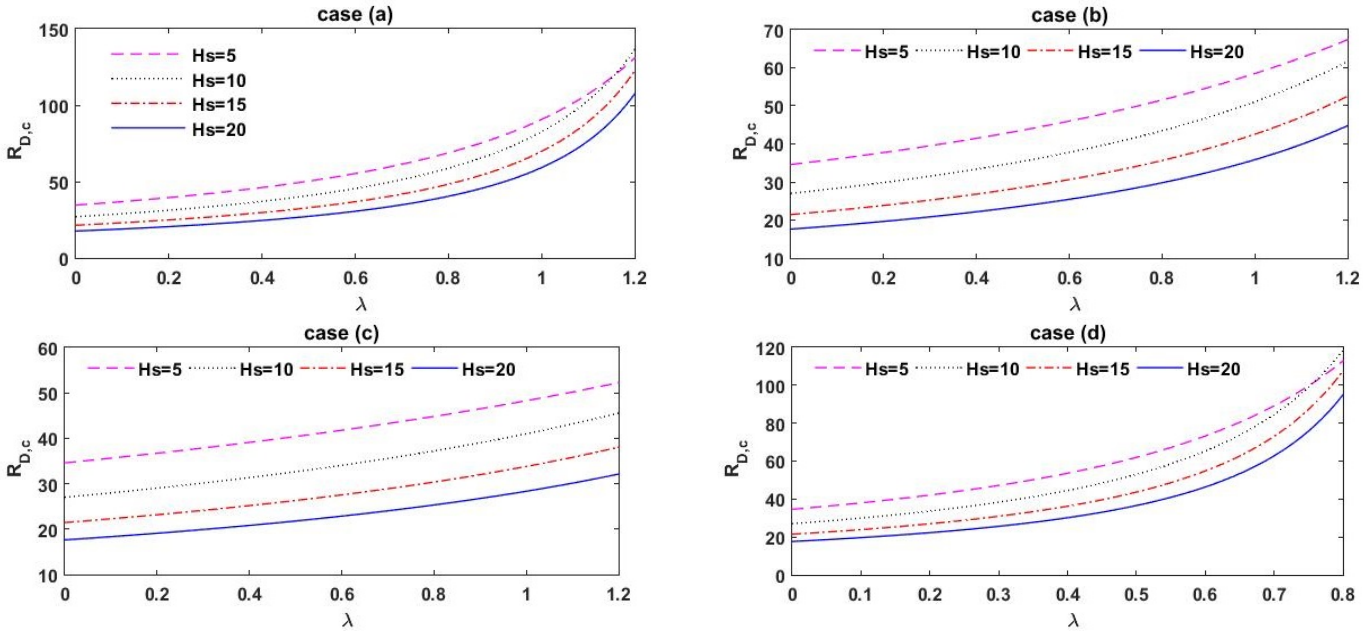

Figure 1. Variation of $R_{D,c}$ with λ for various values of Hs at $\xi = 0.8$ and $\eta = 0.8$ for categories (a) $G(z) = -z$, (b) $G(z) = -z^2$, (c) $G(z) = -z^3$, and (d) $G(z) = -(e^z - 1)$.

Table 2. Estimation of $R_{D,c}$ and a_c for various values of Hs and λ for flow in isotropic porous medium, i.e. $\xi = \eta = 1$ for categories (a) $G(z) = -z$, (b) $G(z) = -z^2$, (c) $G(z) = -z^3$, and (d) $G(z) = -(e^z - 1)$.

		For case: (a)		For case: (b)		For case: (c)		For case: (d)	
Hs	λ	$R_{D,c}$	a_c^2	$R_{D,c}$	a_c^2	$R_{D,c}$	a_c^2	$R_{D,c}$	a_c^2
	0.0	39.478	3.142	39.478	3.142	39.478	3.142	39.478	3.142
	0.2	43.852	3.142	41.832	3.142	40.894	3.142	45.607	3.144
	0.4	49.272	3.145	44.455	3.144	42.398	3.143	53.828	3.153
0	0.6	56.143	3.152	47.389	3.149	43.996	3.146	65.280	3.179
	0.8	65.087	3.166	50.682	3.156	45.694	3.150	81.856	3.247
	1.0	77.080	3.195	54.390	3.168	47.500	3.155	106.293	3.420
	1.2	93.660	3.257	58.576	3.185	49.419	3.163	140.370	3.804
	0.0	34.595	3.421	34.595	3.421	34.595	3.421	34.595	3.421
	0.2	39.549	3.389	37.735	3.386	36.720	3.390	42.099	3.361
	0.4	46.131	3.348	41.473	3.347	39.100	3.357	53.606	3.281
5	0.6	55.281	3.297	45.989	3.304	41.781	3.323	73.234	3.170
	0.8	68.809	3.229	51.536	3.256	44.817	3.287	112.789	3.020
	1.0	90.645	3.137	58.484	3.203	48.278	3.250	216.826	3.000
	1.2	130.905	3.012	67.388	3.144	52.247	3.211	538.607	3.480
	0.0	27.016	3.816	27.016	3.816	27.016	3.816	27.016	3.816
	0.2	31.257	3.781	29.868	3.775	29.029	3.776	33.656	3.747
	0.4	37.062	3.737	33.374	3.727	31.349	3.734	44.522	3.650
10	0.6	45.480	3.677	37.782	3.672	34.049	3.688	65.297	3.501
	0.8	58.749	3.594	43.475	3.609	37.225	3.638	118.378	3.280
	1.0	82.561	3.472	51.082	3.535	41.005	3.586	355.952	3.636
	1.2	136.279	3.289	61.691	3.449	45.567	3.529	1315.364	5.54
	0.0	21.446	4.055	21.446	4.055	21.446	4.055	21.446	4.055
	0.2	24.925	4.022	23.840	4.014	23.165	4.015	26.966	3.988
	0.4	29.739	3.980	26.821	3.967	25.171	3.971	36.233	3.891
15	0.6	36.833	3.922	30.630	3.912	27.537	3.923	54.797	3.739
	0.8	48.291	3.839	35.653	3.847	30.367	3.872	107.480	3.516
	1.0	69.738	3.715	42.550	3.770	33.801	3.816	387.470	3.334
	1.2	122.458	3.527	52.533	3.681	38.043	3.756	1792.891	6.288
	0.0	17.627	4.195	17.627	4.195	17.627	4.195	17.627	4.195
	0.2	20.531	4.163	19.648	4.155	19.091	4.155	22.266	4.129
	0.4	24.572	4.122	22.182	4.108	20.811	4.111	30.155	4.032
20	0.6	30.572	4.064	25.446	4.052	22.854	4.062	46.337	3.877
	0.8	40.381	3.982	29.796	3.986	25.319	4.010	94.904	3.647
	1.0	59.137	3.854	35.854	3.908	28.341	3.953	378.011	4.691
	1.2	107.378	3.657	44.792	3.816	32.118	3.891	2047.480	6.853

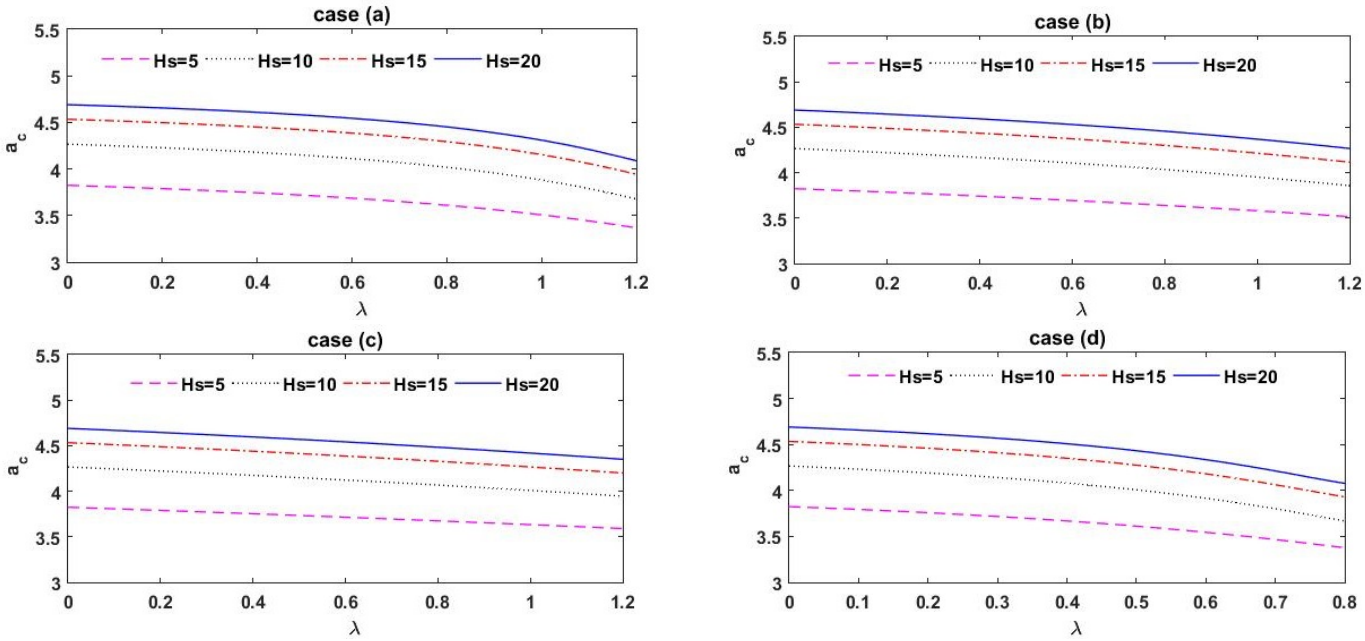

Figure 2. Variation of a_c with λ for various values of Hs at $\xi = 0.8$ and $\eta = 0.8$ for categories (a) $G(z) = -z$, (b) $G(z) = -z^2$, (c) $G(z) = -z^3$, and (d) $G(z) = -(e^z - 1)$.

Table 3. Estimation of $R_{D,c}$ and a_c for various values of Hs and λ at $\xi = 0.8$ and $\eta = 0.7$ for categories (a) $G(z) = -z$, (b) $G(z) = -z^2$, (c) $G(z) = -z^3$, and (d) $G(z) = -(e^z - 1)$.

		For case: (a)		For case: (b)		For case: (c)		For case: (d)	
Hs	λ	$R_{D,c}$	a_c^2	$R_{D,c}$	a_c^2	$R_{D,c}$	a_c^2	$R_{D,c}$	a_c^2
	0.0	36.970	3.632	36.970	3.632	36.970	3.632	36.970	3.632
	0.2	41.065	3.632	39.174	3.632	38.296	3.632	42.709	3.634
	0.4	46.141	3.636	41.630	3.635	39.704	3.634	50.407	3.645
0	0.6	52.576	3.643	44.377	3.640	41.200	3.637	61.132	3.675
	0.8	60.951	3.660	47.461	3.648	42.791	3.641	76.653	3.754
	1.0	72.181	3.694	50.934	3.662	44.481	3.647	99.534	3.954
	1.2	87.706	3.765	54.853	3.682	46.278	3.656	131.438	4.398
	0.0	32.395	3.954	32.395	3.954	33.295	3.954	32.395	3.954
	0.2	37.034	3.917	35.336	3.914	34.385	3.918	39.423	3.886
	0.4	43.199	3.871	38.837	3.869	36.614	3.881	50.200	3.793
5	0.6	51.768	3.811	43.066	3.819	39.125	3.841	68.584	3.665
	0.8	64.438	3.733	48.261	3.764	41.969	3.800	105.634	3.491
	1.0	84.891	3.626	54.769	3.702	45.211	3.757	202.849	3.345
	1.2	122.602	3.481	63.109	3.635	48.928	3.712	504.493	3.023
	0.0	25.297	4.411	25.297	4.411	25.297	4.411	25.297	4.411
	0.2	29.268	4.371	27.968	4.364	27.182	4.366	31.515	4.332
	0.4	34.704	4.320	31.251	4.309	29.355	4.316	41.691	4.219
10	0.6	42.588	4.251	35.379	4.246	31.883	4.263	61.149	4.047
	0.8	55.015	4.155	40.711	4.172	34.858	4.206	110.870	3.791
	1.0	77.318	4.013	47.836	4.086	38.399	4.145	333.404	4.203
	1.2	127.637	3.802	57.773	3.987	42.672	4.080	1231.986	6.412
	0.0	20.081	4.688	20.081	4.688	20.081	4.688	20.081	4.688
	0.2	23.338	4.650	22.323	4.641	21.691	4.641	25.250	4.611
	0.4	27.847	4.601	25.115	4.586	23.569	4.591	33.929	4.498
15	0.6	34.491	4.534	28.682	4.522	25.785	4.535	51.315	4.322
	0.8	45.221	4.438	33.386	4.447	28.436	4.476	100.663	4.064
	1.0	65.309	4.294	39.846	4.358	31.652	4.411	362.920	5.011
	1.2	114.691	4.077	49.196	4.255	35.625	4.342	1679.313	7.268
	0.0	16.504	4.850	16.504	4.850	16.504	4.850	16.504	4.850
	0.2	19.224	4.813	18.398	4.803	17.876	4.803	20.849	4.774
	0.4	23.008	4.765	20.771	4.749	19.486	4.752	28.237	4.661
20	0.6	28.628	4.699	23.828	4.685	21.400	4.696	43.393	4.482
	0.8	37.814	4.603	27.901	4.608	23.708	4.635	88.886	4.215
	1.0	55.280	4.455	33.575	4.518	26.539	5.569	354.049	5.422
	1.2	100.568	4.227	41.947	4.411	30.076	4.498	1917.791	7.921

It is found that the gravity variation parameter λ delays on the onset of convection, while an opposite trend is noticed with increasing internal heating parameter Hs. This is because the heat supply of the system increases with rising Hs which eventually directs to decline in the value of $R_{D,c}$. The critical thermal Rayleigh-Darcy number $R_{D,c}$ supplements upon rising gravity variation parameter λ. This is because the gravity variation parameter reduces the strength of gravity force. Consequently, the frustration in the arrangement returns and this leads to holdup the start of convection. The size of the convection cells decreased with Hs while it augmented with λ.

Furthermore, it is seen that the scheme shows more instability for category (c), while it is maximum stable for category (d). For big estimates of λ ($\lambda \geq 1$), from Tables 2 and 3, it is attractive to note that the consequence of Hs is reverse on $R_{D,c}$, whereas the effect of λ is reverse on a_c.

To see the power of ξ on the stability of the arrangement, $R_{D,c}$ and a_c are sketched in Figs. 3 and 4 as a function of λ for

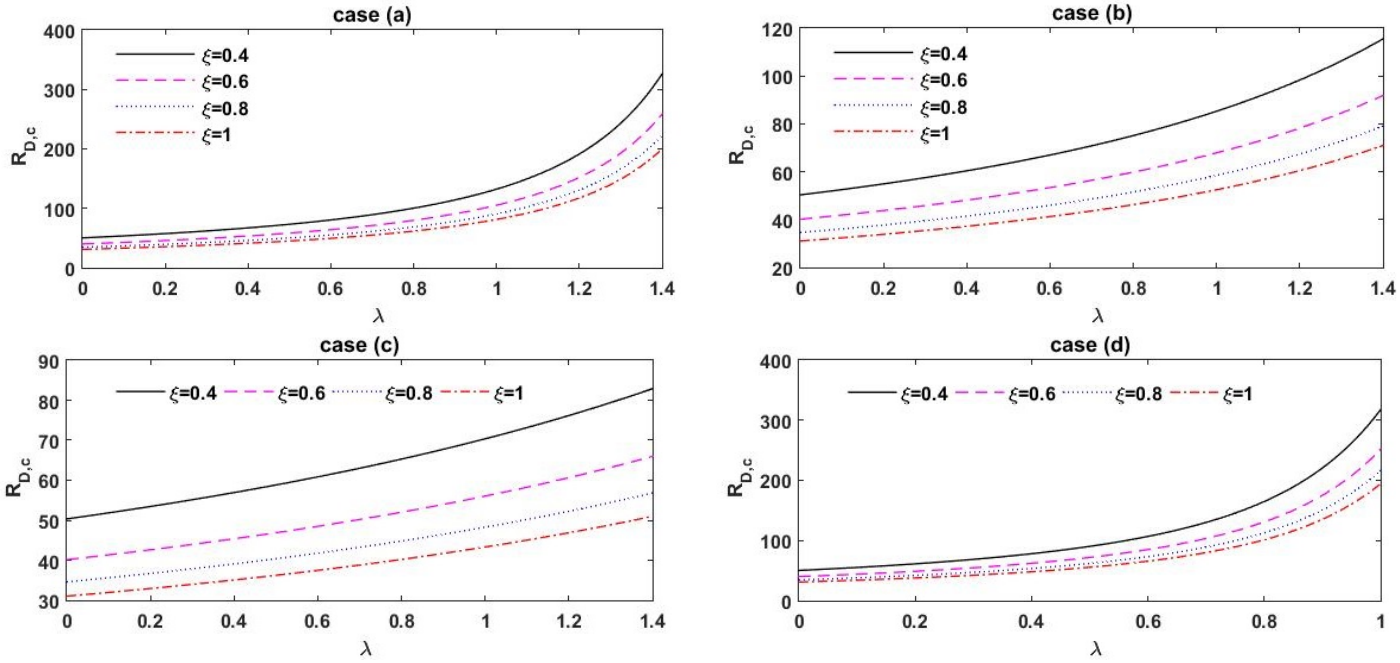

Figure 3. Variation of $R_{D,c}$ with λ for various values of ξ at Hs $= 5$ and $\eta = 0.8$ for categories (a) $G(z) = -z$, (b) $G(z) = -z^2$, (c) $G(z) = -z^3$, and (d) $G(z) = -(e^z - 1)$.

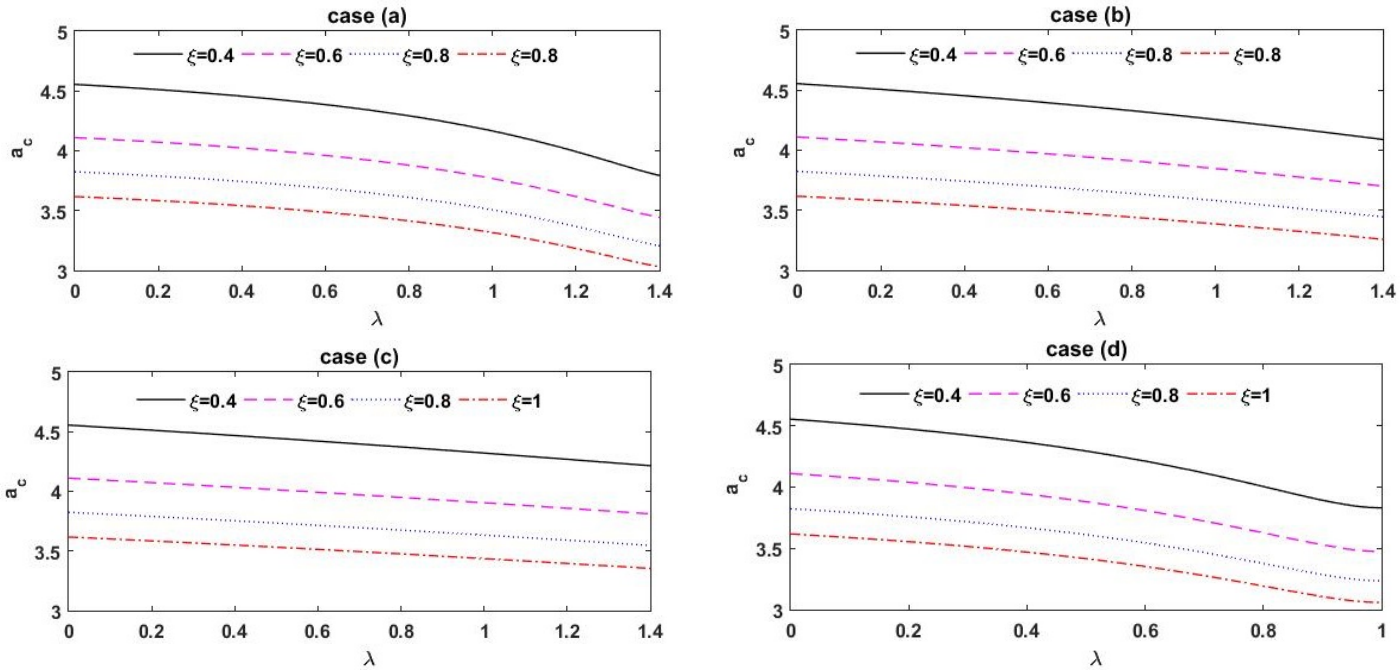

Figure 4. Variation of a_c with λ for various values of ξ at Hs $= 5$ and $\eta = 0.8$ for categories (a) $G(z) = -z$, (b) $G(z) = -z^2$, (c) $G(z) = -z^3$, and (d) $G(z) = -(e^z - 1)$.

diverse values of ξ. The consequences are also summarized in Table 4. We showed that the outcome of rising ξ hurries the beginning of convection. This is because the effect of increasing ξ leads to bigger horizontal permeability which accelerates the activity of the liquid in the horizontal path and thus lesser estimates of $R_{D,c}$ are required for the start of convection with increasing ξ. From Fig. 4, the critical wave number a_c reduces as ξ increased and so its outcome is to enlarge the dimension of convection cells. This happened because the low confrontation to horizontal flow also directs to an expansion of the horizontal wavelength.

The effect of η on the stability of the scheme is completed in Figs. 5 and 6, and also listed in Table 5.

From these, it is established that $R_{D,c}$ amplifies on amplify in the rate of the thermal anisotropy parameter η, while a_c decreases on increasing η. This shows that the thermal anisotropy parameter η has a stabilizing consequence on the stability of the arrangement. This is for the reason that the horizontal thermal diffusivity enlarges with η.

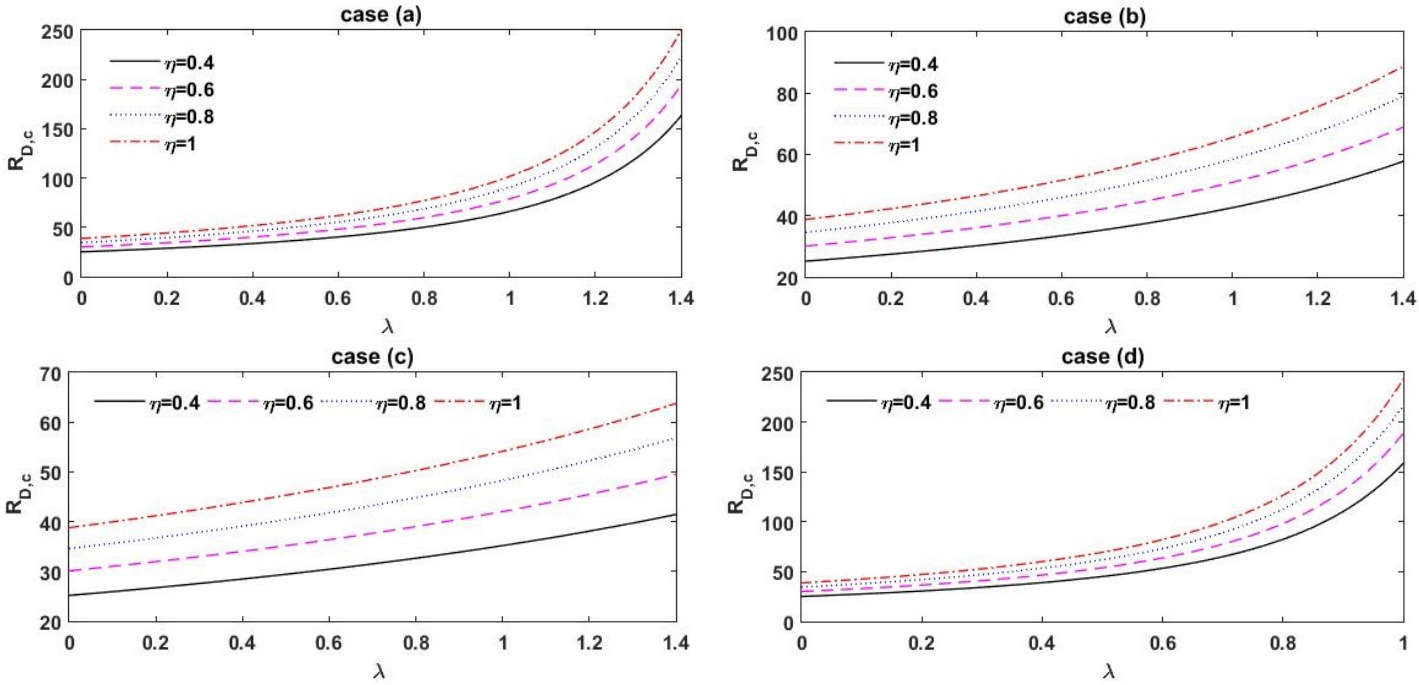

Figure 5. Variation of $R_{D,c}$ with λ for various values of η at Hs = 5 and $\xi = 0.8$ for categories (a) $G(z) = -z$, (b) $G(z) = -z^2$, (c) $G(z) = -z^3$, and (d) $G(z) = -(e^z - 1)$.

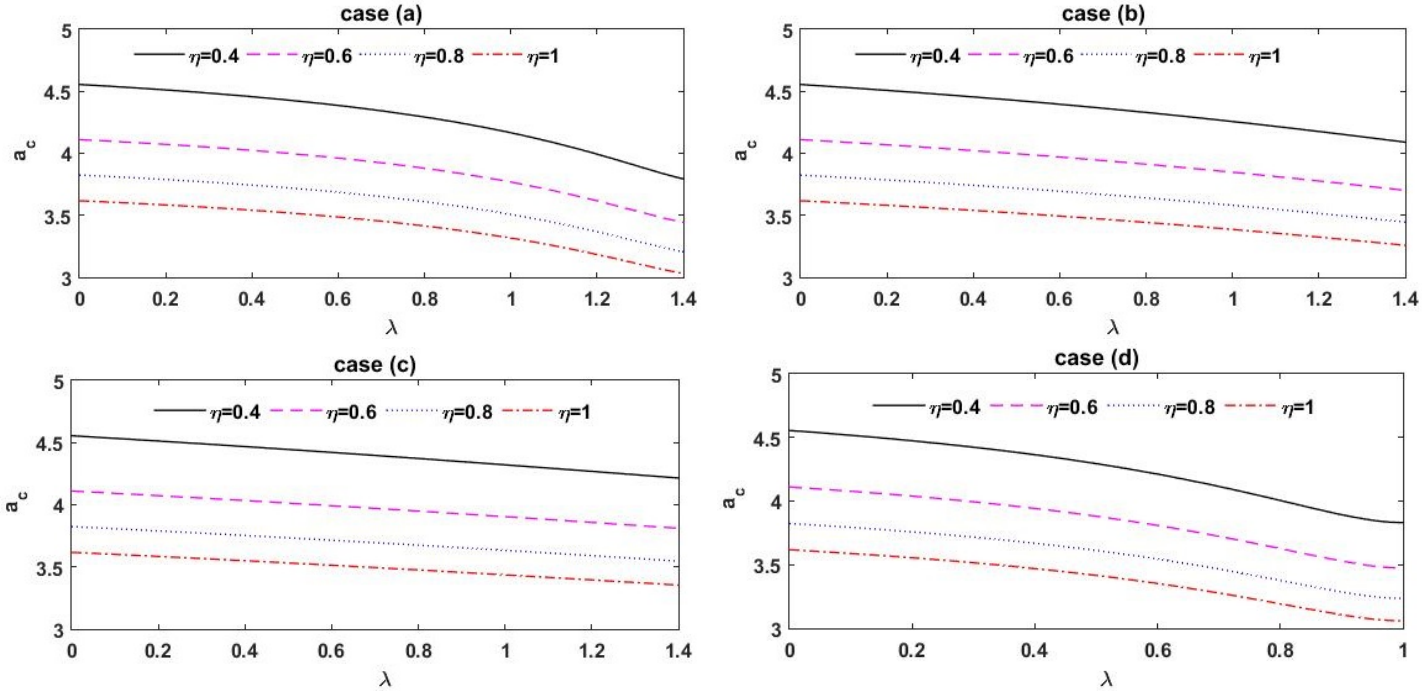

Figure 6. Variation of a_c with λ for various values of η at Hs = 5 and $\xi = 0.8$ for categories (a) $G(z) = -z$, (b) $G(z) = -z^2$, (c) $G(z) = -z^3$, and (d) $G(z) = -(e^z - 1)$.

Table 4. Estimation of $R_{D,c}$ and a_c for various values of ξ and λ at Hs = 5 and $\eta = 0.8$ for categories (a) $G(z) = -z$, (b) $G(z) = -z^2$, (c) $G(z) = -z^3$, and (d) $G(z) = -(e^z - 1)$.

		For case: (a)		For case: (b)		For case: (c)		For case: (d)	
ξ	λ	$R_{D,c}$	a_c^2	$R_{D,c}$	a_c^2	$R_{D,c}$	a_c^2	$R_{D,c}$	a_c^2
	0.0	50.340	4.555	50.340	4.555	50.340	4.555	50.340	4.555
	0.2	57.565	4.511	54.926	4.508	53.445	4.513	61.293	4.474
	0.4	67.172	4.456	60.389	4.455	56.927	4.468	78.109	4.364
0.4	0.6	80.538	4.386	66.992	4.395	60.849	4.421	106.839	4.212
	0.8	100.320	4.293	75.109	4.330	65.294	4.372	164.867	4.005
	1.0	132.300	4.166	85.285	4.256	70.363	4.321	317.437	3.831
	1.2	191.375	3.993	98.336	4.176	76.178	4.269	789.390	4.623
	0.0	40.144	4.111	40.144	4.111	40.144	4.111	40.144	4.111
	0.2	45.895	4.072	43.791	4.069	42.612	4.073	48.857	4.039
	0.4	53.537	4.024	48.132	4.022	45.376	4.034	62.220	3.942
0.6	0.6	64.162	3.961	53.376	3.970	48.490	3.992	85.019	3.808
	0.8	79.873	3.879	59.819	3.912	52.018	3.949	130.984	3.627
	1.0	105.241	3.768	67.891	3.847	56.038	3.904	251.623	3.475
	1.2	152.027	3.617	78.236	3.777	60.649	3.858	625.788	4.180
	0.0	34.595	3.824	34.595	3.824	34.595	3.824	34.595	3.824
	0.2	39.549	3.789	37.735	3.785	36.720	3.790	42.099	3.758
	0.4	46.131	3.744	41.473	3.742	39.100	3.753	53.606	3.668
0.8	0.6	55.281	3.686	45.989	3.694	41.781	3.715	73.234	3.545
	0.8	68.809	3.610	51.536	3.640	44.817	3.675	112.789	3.376
	1.0	90.645	3.507	58.484	3.581	48.278	3.633	216.565	3.236
	1.2	130.905	3.367	67.388	3.515	52.247	3.591	538.607	3.891
	0.0	31.035	3.617	31.035	3.617	31.035	3.617	31.035	3.617
	0.2	35.480	3.583	33.853	3.581	32.942	3.584	37.769	3.554
	0.4	41.386	3.541	37.208	3.540	35.078	3.550	48.096	3.469
1.0	0.6	49.598	3.486	41.261	3.494	37.484	3.514	65.715	3.352
	0.8	61.740	3.414	46.239	3.443	40.210	3.476	101.229	3.192
	1.0	81.342	3.317	52.477	3.386	43.317	3.436	194.426	3.059
	1.2	117.490	3.184	60.471	3.324	46.880	3.396	483.542	3.679

Table 5. Estimation of $R_{D,c}$ and a_c for various values of η and λ at Hs = 5 and $\xi = 0.8$ for categories (a) $G(z) = -z$, (b) $G(z) = -z^2$, (c) $G(z) = -z^3$, and (d) $G(z) = -(e^z - 1)$.

		For case: (a)		For case: (b)		For case: (c)		For case: (d)	
η	λ	$R_{D,c}$	a_c^2	$R_{D,c}$	a_c^2	$R_{D,c}$	a_c^2	$R_{D,c}$	a_c^2
	0.0	25.170	4.555	25.170	4.555	25.170	4.555	25.170	4.555
	0.2	28.783	4.511	27.463	4.508	26.723	4.513	30.647	4.474
	0.4	33.586	4.456	30.195	4.455	28.463	4.468	39.055	4.364
0.4	0.6	40.269	4.386	33.496	4.395	30.425	4.421	53.420	4.212
	0.8	50.160	4.293	37.555	4.330	32.647	4.372	82.433	4.005
	1.0	66.150	4.166	42.643	4.256	35.181	4.321	158.718	3.831
	1.2	95.688	3.993	49.168	4.176	38.089	4.269	394.695	4.623
	0.0	30.108	4.111	30.108	4.111	30.108	4.111	30.108	4.111
	0.2	34.422	4.072	32.843	4.069	31.959	4.073	36.643	4.039
	0.4	40.153	4.024	36.099	4.022	34.032	4.034	46.665	3.942
0.6	0.6	48.122	3.961	40.032	3.970	36.367	3.992	63.765	3.808
	0.8	59.905	3.879	44.864	3.912	39.013	3.949	98.238	3.627
	1.0	78.931	3.768	50.918	3.847	42.028	3.904	188.717	3.475
	1.2	114.020	3.617	58.677	3.777	45.487	3.858	469.341	4.180
	0.0	34.595	3.824	34.595	3.824	34.595	3.824	34.595	3.824
	0.2	39.549	3.789	37.735	3.785	36.720	3.790	42.099	3.758
	0.4	46.131	3.744	41.473	3.742	39.100	3.753	53.606	3.668
0.8	0.6	55.281	3.686	45.989	3.694	41.781	3.715	73.234	3.545
	0.8	68.809	3.610	51.536	3.640	44.817	3.675	112.789	3.376
	1.0	90.645	3.507	58.484	3.581	48.278	3.633	216.565	3.236
	1.2	130.905	3.367	67.388	3.515	52.247	3.591	538.607	3.891
	0.0	38.794	3.617	38.794	3.617	38.794	3.617	38.794	3.617
	0.2	44.350	3.583	42.316	3.581	41.177	3.584	47.211	3.554
	0.4	51.733	3.541	46.510	3.540	43.847	3.550	60.120	3.469
1.0	0.6	61.998	3.486	51.576	3.494	46.855	3.514	82.144	3.352
	0.8	77.175	3.414	57.799	3.443	50.263	3.476	126.536	3.192
	1.0	101.678	3.317	65.596	3.386	54.146	3.436	243.032	3.059
	1.2	146.863	3.184	75.588	3.324	58.600	3.396	604.427	3.679

VI. SUMMARY

The influence of the consistent internal heat source and the uneven gravity force on the launch of convective activity in an anisotropic porous layer was presented numerically. The investigation was provided for four types of gravity field digression: (a)$G(z) = -z$, (b) $G(z) = -z^2$, (c) $G(z) = -z^3$, and (d) $G(z) = -(e^z - 1)$. The major conclusions of the current investigation are as follows.

- The system was found to be more stable on increasing η and λ, whereas it was more unstable on increasing ξ and Hs.
- The measurement of the convection cells decreased on raising the internal heating parameter Hs, while it increased with ξ, η and λ.
- For huge values of gravity variation parameter λ ($\lambda \geq 1$), the effect of Hs was opposite on $R_{D,c}$, while the effect of λ was opposite on a_c.
- The system shows more instability for category (c), while it is more stable for category (d).

ACKNOWLEDGMENTS

The author wish to thank the administration of University of Nizwa for continous support during this research.

BIBLIOGRAPHY

[1] P. Cheng, Adv. Heat Transfer **14**, 1 (1979).
[2] C. Doughty and K. Pruess, Int. J. Heat Mass Transfer **31**, 79 (1988).
[3] N. Khoshnevis, R. Khosrokhavar, H. M. Nick, D. F. Bruhn, and H. Bruining, J. Pet. Sci. Eng. **178**, 616 (2019).
[4] V. Rakesh and A. K. Datta, AIChE J. **59**, 33 (2013).
[5] D. Holton, S. Myers, G. Carta, A. Hoch, M. Dickinson, and N. Carr, Eng. Geol. **211**, 102 (2016).
[6] A. Barletta, M. Celli, and M. Ouarzazi, Int. J. Therm. Sci. **120**, 427 (2017).
[7] C. Horton and F. Rogers Jr, J. Appl. Phys. **16**, 367 (1945).
[8] D. A. Nield and A. Bejan, Convection in porous media, vol. 3 (Springer, 2006).
[9] G. Castinel and M. Combarnous, CR Acad. Sci. B **278**, 701 (1974).
[10] J. Epherre, Rev. Gen. Thermique **168**, 949 (1975).
[11] O. Kvernvold and P. A. Tyvand, J. Fluid Mech. **90**, 609 (1979).
[12] G. Degan, P. Vasseur, and E. Bilgen, Int. J. Heat Mass Transfer **38**, 1975 (1995).
[13] L. Payne, J. Rodrigues, and B. Straughan, Math. Method. Appl. Sci. **24**, 427 (2001).
[14] D. Rees and A. Postelnicu, Int. J. Heat Mass Transfer **44**, 4127 (2001).
[15] S. Govinder, Transp. Porous Media **69**, 55 (2007).
[16] M. S. Malashetty and M. Swamy, Int. J. Therm. Sci. **49**, 867 (2010).
[17] D. Yadav and M. C. Kim, J. Porous Media **17**, 1061 (2014).
[18] I. S. Shivakumara, A. L. Mamatha, and M. Ravisha, Appl. Math. Comput. **259**, 838 (2015).
[19] A. Mahajan and R. Nandal, Int. J. Heat Mass Transfer **115**, 235 (2017).
[20] R. Gasser and M. Kazimi, J. Heat Transfer **98**, 49 (1976).
[21] C. Parthiban and P. R. Patil, Int. Commun. Heat Mass Transfer **24**, 1049 (1997).
[22] A. Nouri-Borujerdi, A. R. Noghrehabadi, and D. A. S. Rees, Int. J. Therm. Sci. **47**, 1020 (2008).
[23] B. Bhadauria, A. Kumar, J. Kumar, N. C. Sacheti, and P. Chandran, Transp. Porous Media **90**, 687 (2011).
[24] L. Storesletten and D. A. S. Rees, Fluids **4**, 75 (2019).
[25] D. Yadav, R. Bhargava, and G. S. Agrawal, Int. J. Therm. Sci. **60**, 244 (2012).
[26] D. Yadav and J. Wang, Heat Transfer Eng. **40**, 1363 (2018).
[27] R. Chand, D. Yadav, and G. Rana, Int. J. Nanoparticles **8**, 241 (2015).
[28] D. Yadav, C. Kim, J. Lee, and H. H. Cho, Comput. Fluids **121**, 26 (2015).
[29] D. Yadav, J. Appl. Fluid Mech. **10**, 763 (2017).
[30] D. Yadav, Int. J. Appl. Comput. Math. **3**, 3663 (2017).
[31] D. Yadav, J. Wang, and J. Lee, J. Porous Media **20**, 691 (2017).
[32] D. Yadav, J. Therm. Anal. Calorim. **135**, 1107 (2019).
[33] A. Mahajan and M. K. Sharma, Phys. Fluids **29**, 034101 (2017).
[34] A. Khalili and I. Shivakumara, Phys. Fluids **10**, 315 (1998).
[35] D. Nield and A. Kuznetsov, Transp. Porous Media **99**, 73 (2013).
[36] C. Hirt, S. Claessens, T. Fecher, M. Kuhn, R. Pail, and M. Rexer, Geophys. Res. Lett. **40**, 4279 (2013).
[37] B. D. Tapley, S. Bettadpur, J. C. Ries, P. F. Thompson, and M. M. Watkins, Science **305**, 503 (2004).
[38] S. M. Alex and P. R. Patil, Int. Commun. Heat Mass Transfer **28**, 509 (2001).
[39] Q. Li, J. Wang, J. Wang, J. Baleta, C. Min and B. Sundén, Energ. Convers. Manage. **171**, 1440 (2018).
[40] P. Kaloni and Z. Qiao, Int. J. Heat Mass Transfer **44**, 1585 (2001).
[41] S. M. Alex and P. R. Patil, J. Porous Media **5**, 11 (2002).
[42] S. M. Alex, P. R. Patil, and K. Venkatakrishnan, Fluid Dyn. Res. **29**, 1 (2001).
[43] S. M. Alex and P. R. Patil, J. Heat Transfer **124**, 144 (2002).
[44] S. Rionero and B. Straughan, Int. J. Eng. Sci. **28**, 497 (1990).
[45] A. Harfash, Transp. Porous Media **103**, 361 (2014).
[46] A. Mahajan and M. K. Sharma, Appl. Math. Comput. **339**, 622 (2018).
[47] R. Chand, G. Rana, and S. Kango, FME Trans. **43**, 62 (2015).
[48] D. Yadav, Heat Tran. Asian Res. **49**, 1170 (2020).
[49] D. Yadav, Int. Commun. Heat Mass Transfer **108**, 104274 (2019).
[50] D. Yadav, J. Appl. Comput. Mech. **6**, 699 (2020).
[51] L. Cordell, Geophys. **38**, 684 (1973).

[52] A. J. Shneiderov, Trans. Am. Geophys.Union **24**, 61 (1943).
[53] L. Shi, Y. Li, and E. Zhang, J. Appl. Geophys. **116**, 1 (2015).
[54] R. McKibbin, Transp. Porous Media **1**, 271 (1986).
[55] I. S. Shivakumara and M. Dhananjaya, Ain Shams Eng. J. **6**, 703 (2015).
[56] S. Chandrasekhar, Hydrodynamic and Hydromagnetic Stability, (Dover Publication, 2013).
[57] D. Yadav, Heat Transfer Asian Res. (2020) DOI: 10.1002/htj.21767
[58] D. Yadav and M. Maqhusi, Asia-Pac. J. Chem. Eng. (2020) DOI: 10.1002/apj.2514
[59] D. Yadav, Rev. Cubana Fis. **35**, 108 (2018).
[60] D. Yadav and J. Lee, J. Appl. Fluid Mech. **2**, 519 (2016).
[61] D. Yadav, R. Bhargava, G. S. Agrawal, G. S. Hwang, J. Lee and M. C. Kim, Asia-Pac. J. Chem. Eng. **9**, 663 (2014)
[62] D. Yadav, R. Bhargava, G. S. Agrawal, N. Yadav, J. Lee and M. C. Kim, Microfluid. Nanofluid. **16**, 425 (2016).
[63] G. C. Rana, R. Chand and V. Sharma, Rev. Cubana Fis. **33**, 89 (2016).